Mn overlayers on PbTe (111): Substitutional adsorption and interface formation*

Wu Hai-Fei(吴海飞)[a)b)], Zhang Han-Jie(张寒洁)[a)], Lu Yun-Hao(陆赟豪)[c)], Yan Yong-Hong(鄢永红)[b)], Li Hai-Yang(李海洋)[a)], Bao Shi-Ning(鲍世宁)[a)], and He Pi-Mo(何丕模)[a)†]

[a)] *Department of Physics, Zhejiang University, Hangzhou* 310027, *China*
[b)] *Department of Physics, Shaoxing University, Shaoxing* 312000, *China*
[c)] *Department of Materials Science and Engineering, Zhejiang University, Hangzhou* 310027, *China*

(Received 22 April 2014; revised manuscript received 31 July 2014; published online 10 October 2014)

The formation of the Mn/PbTe (111) interface is investigated by photoemission spectrum. The core level behavior of Mn 2p is consistent with Mn substitutional adsorption during the initial Mn deposition, forming a $(\sqrt{3}\times\sqrt{3})R30°$-$Pb_{0.67}Mn_{0.33}Te$ phase of the second layer. Further deposition of Mn can cause metallic Mn islands to cover the substitutional substrate. Ultraviolet photoemission measurements show that the Fermi level is shifted into the conduction band, indicating Ohmic contact formation at the Mn/PbTe (111) interface. The valence band maximum associated with the $Pb_{0.67}Mn_{0.33}Te$ layer is located at 1.27 eV below the Fermi level, and a schematic electronic structure of the Mn/PbTe (111) interface is given. The work function of the substituted substrate with Pb-covered Mn islands is determined to be 4.16 eV, in comparison with 4.35 eV for the Pb-covered substituted substrate and 3.95 eV for the pristine PbTe (111) surface.

Keywords: photoemission spectrum, metal–semiconductor, electronic structure, PbTe

PACS: 79.60.–I, 79.60.Jv, 73.30.+y, 73.20.At **DOI:** 10.1088/1674-1056/23/12/127901

1. Introduction

Narrow band-gap PbTe is of great interest for its thermoelectric and optical properties and important applications in energy and light sources.[1–4] The mobility values of electrons and holes in PbTe are strongly influenced by magnetic dopants. Many interesting properties, such as magneto–optical effects related to the giant Zeeman splitting of band states,[5] carrier-induced ferromagnetism,[6] and the formation of bound magnetic polarons,[7] occur in magnetic element-doped PbTe. An important property was recently discovered that the thermoelectric power of $Pb_{1-x}Mn_xTe$ is about twice as high as that of pure PbTe.[8] Although it is speculated that the various properties of magnetic element-doped PbTe mainly originate from the sp–d exchange interaction between the delocalized band carriers and the localized magnetic moments introduced into the host lattice by the magnetic ions, the detailed mechanism of the exchange interaction between the host material and magnetic dopants is still unclear.

Up to now, most studies have concentrated on the bulk PbTe system,[9,10] and a few of them have focused on the interaction between the magnetic atoms and the surface of PbTe, which is another way to explore the interaction between magnetic atoms and host materials. This is also very important for PbTe, for it has been used not only as bulk but also as films,[11,12] quantum wells,[13] superlattices,[14] nanowires,[15] and colloidal and embedded nanocrystals.[16] Recently, it has been reported that PbTe is converted from a normal insulator into a nontrivial topological insulator under surface strain,[17] and that the surface state, which is protected by time reversal symmetry, can be engineered only by magnetic adsorbate.[18] Moreover, the investigation of the initial growth of dopant on the surface is helpful to formulate a microscopic picture for the incorporation of dopant into bulk materials.[19,20]

Manganese (Mn) is the most common magnetic dopant for PbTe.[21] It is believed that its outermost $4s^2$ electrons contribute to the crystal bonds while the $3d^5$ electrons stay localized. The total spin of the Mn^{2+} ion is 5/2 and its total orbital momentum L is zero. Therefore, in the absence of an external magnetic field, the ground state of the Mn ion is sixfold-spin degenerate, and there is no crystal field effect on it due to the vanishing angular momentum.[22] In this work, we systemically study the adsorption of Mn on the PbTe (111) surface by using photoemission spectrum.

2. Experimental details

The experiments were performed in a multifunctional ultrahigh-vacuum (UHV) VT-SPM system (Omicron Instruments for Surface Science) with a base pressure better than 2×10^{-10} Torr (1 Torr = 1.33322×10^2 Pa). The system was

*Project supported by the National Natural Science Foundation of China (Grant Nos. 11074214, 51202149, and 11204180), the Natural Science Foundation of Zhejiang Province, China (Grant No. LQ12F04001), the Scientific Research Fund of Zhejiang Provincial Education Department, China (Grant No. Y201121234), and the Ministry of Science and Technology of China.

†Corresponding author. E-mail: phypmhe@dial.zju.edu.cn

© 2014 Chinese Physical Society and IOP Publishing Ltd

described in detail elsewhere.[23] PbTe (111) film (∼ 1-μm thick) was *ex situ* grown by molecular beam epitaxy (MBE) on the BaF_2 (111) substrate in a solid source MBE system.[24] Once it was transferred to the multifunctional UHV VT-SPM system, a clean ordered PbTe (111) surface was obtained by Ar^+ (500 eV) sputtering for 1 h, followed by annealing at 250 °C for 10 min. The cleanliness and the orientation of the sample were checked by low-energy electron diffraction (LEED) and subsequent X-ray photoemission spectrum (XPS) measurement, and a sharp (1×1) LEED pattern was observed after the surface had been cleaned, which has previously been determined to be the Pb-terminated surface.[23] Mn was deposited from a resistance-heating Mn evaporator. The thickness values of the deposited layers were monitored using a quartz crystal oscillator, and calibrated with the XPS measurements. The deposition rate was controlled at about 0.15 monolayer (ML)/min, and during deposition the temperature of the PbTe (111) substrate was kept at room temperature. The XPS measurements were carried out with an Mg Kα source (1253.6 eV), and the resolution of the peak shift for XPS measurements was estimated to be about 0.13 eV. The ultraviolet photoemission spectrum (UPS) measurements were performed with a He–I (21.2 eV) UV lamp and a sample bias of −5.0 V. The overall energy resolution for UPS was about 0.15 eV. All the XPS and UPS measurements were carried out at room temperature.

3. Results and discussion

3.1. XPS measurements for Mn overlayer on PbTe (111)

Figure 1 shows the XPS spectra of Mn 2p core level collected each as a function of Mn thickness for Mn deposition on the Pb-terminated PbTe (111) surface. It is worth mentioning that the peak at 644.5 eV (denoted by *C*) for the clean PbTe (111) surface originates from Pb $4p_{3/2}$ core level. As shown in Fig. 1, two new peaks appear at the initial deposition of Mn. These two new peaks, which are located at 641.2 eV (denoted by *B*) and 652.9 eV (marked by *B*′), are ascribed to the Mn $2p_{3/2}$ emission and Mn $2p_{1/2}$ emission, respectively. These spin–orbit-split spectral features are associated with the strong hybridization between the Mn 3d and Te 5p orbitals, indicating the formation of Mn–Te bond, or $Pb_{1-x}Mn_xTe$ compound. Similar results were also observed for Mn deposition on ZnSe, or ZnS, forming $Zn_{1-x}Mn_xSe$,[25] or $Zn_{1-x}Mn_xS$,[26] and more recently at the Mn/CdTe (110) interface.[27] By increasing Mn thickness, the intensities of these Mn–Te bond spectral features (marked by *B* and *B*′ in Fig. 1) increase, and reach their maximum values at a (nominal) Mn thickness of about 0.45 ML.

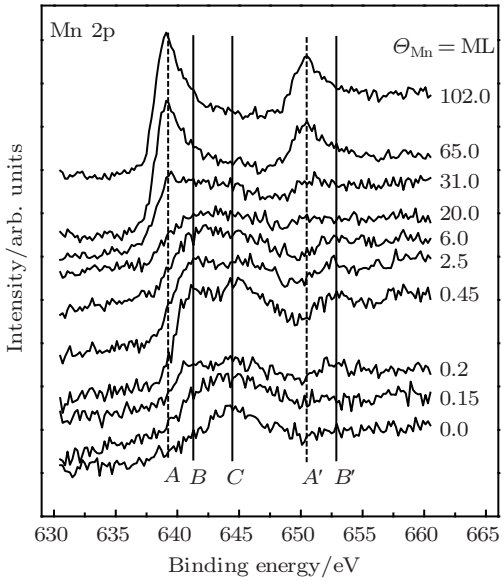


Fig. 1. XPS spectra of the Mn 2p core level each as a function of Mn thickness on PbTe (111). The substrate Pb $4p_{3/2}$ feature at 644.5 eV is denoted by *C*, the spin–orbit-split metallic Mn core levels at 639.2 eV and 650.5 eV are represented by *A* and *A*′, and the spin–orbit-split Mn–Te bond spectral features are marked with *B* and *B*′.

The evolutions of the Mn core level spectra with Mn thickness increasing from zero to 0.45 ML can be understood with our previous investigations for Mn adsorption on PbTe (111).[23,28] The first-principles calculations at the Mn/PbTe (111) interface,[28] together with scanning tunneling microscopy (STM) and XPS measurements of Pb 4f and Te 3d core levels,[23] have already revealed that at the initial deposition of Mn ($\Theta_{Mn} \leq 0.45$ ML) on the Pb-terminated PbTe (111) surface, Mn atoms substitute for the Pb atoms in the 2nd layer by 'kicking them out' from the subsurface (exchange interaction), and bond to the nearby Te ions through the strong hybridization between the Mn 3d and Te 5p orbitals, forming $(\sqrt{3}\times\sqrt{3})R30°$ ($(\sqrt{3}\times\sqrt{3})R30°$-$Pb_{0.67}Mn_{0.33}Te$) superstructure, and the 'kicked out' Pb atoms are released to the top of the surface as free Pb atoms. Accordingly, the schematic structures of this substitutional adsorption of Mn are summarized in Fig. 2. During the initial deposition of Mn, Mn atoms substitute for the 2nd layer Pb atoms, forming Mn substituted $(\sqrt{3}\times\sqrt{3})R30°$ islands, and the 'kicked out' Pb atoms are released to the top of the surface. At an Mn coverage of about 0.45 ML, a full Mn substituted $Pb_{0.67}Mn_{0.33}Te$ layer, i.e. the second layer is formed with 0.33 ML of Pb floating on the top of the surface. Such kinds of exchange (interaction) phenomena between the adatoms and substrate atoms are well-known in III–V, II–VI or V semiconductor heterostructures. In a B/Si (111) system, boron adatoms are substituted for subsurface Si atoms, forming a $(\sqrt{3}\times\sqrt{3})R30°$ superstructure,[29] and for the Mn/GaAs system, Mn adatoms are substituted for Ga atoms, by removing the Ga atoms from the substitutional sites.[30]

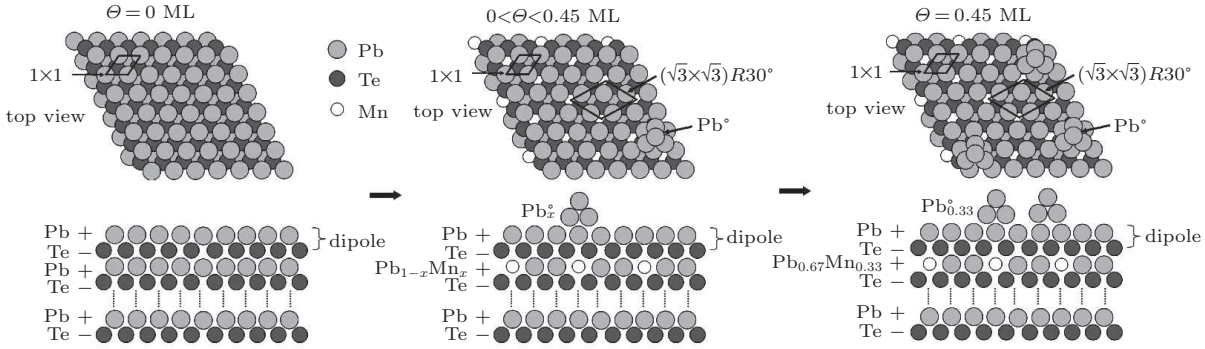


Fig. 2. Schematic structures for substitutional adsorption of Mn. The clean Pb-terminated PbTe (111) substrate is composed of the Pb–Te dipole layer. At a Mn thickness of $\Theta_{\mathrm{Mn}} \leq 0.45$ ML, Mn is substituted for the Pb atoms in the 2nd layer, forming an Mn substitutional $(\sqrt{3}\times\sqrt{3})R30^\circ$ superstructure, and the substituted Pb atoms are released to the top of the surface as free Pb atoms.

Further deposition of Mn with the thickness being larger than 0.45 ML causes the spin–orbit-split metallic Mn core levels to appear at 639.2 eV and 650.5 eV (marked by A and A' in Fig. 1).[27] By increasing the Mn thickness, the intensity of these metallic Mn core levels increases very slowly, and it does not exceed the Mn–Te bond spectral features until the Mn thickness increases up to 31 ML. In addition, the intensity of Pb $4f_{7/2}$ core level at 136.9 eV associated with the free Pb atoms keeps constant up to a Mn thickness of about 102 ML (see Fig. 4(a) in Ref. [23]), far beyond the escape depth of the photoelectron. These results suggest that further deposited Mn atoms ($\Theta_{\mathrm{Mn}} > 0.45$ ML) nucleate on the substitutional surface as metallic Mn islands covered with free Pb atoms on top of the surface, which is in good agreement with the STM results.[23]

3.2. UPS measurements for Mn overlayer on PbTe (111)

In order to further understand the nature of the Mn/PbTe (111) interface, a complete set of UPS measurements are performed. Figure 3 shows the valence-band evolution with Mn thickness, the left panel contains valence-band structures, and the right panel shows the cutoff energy of photoemissions.

During the initial deposition of Mn ($\Theta_{\mathrm{Mn}} \leq 0.45$ ML), the valence-band maximum (VBM) (marked by A in Fig. 3), which is ascribed to pristine PbTe and composed of 5p orbitals of Te and 6s orbitals of Pb,[31] exhibits almost no shift, except for the intensity decrease with the increase of the Mn thickness, which indicates that no band bending occurs for the substitutional adsorption. Meanwhile, an additional VBM appears at about 1.27 eV below the Fermi level (marked by B in Fig. 3), which is ascribed to the 3d-orbitals of Mn atoms and composed of 5p-orbitals of Te atoms (more details will be discussed below). With Mn thickness being about 0.45 ML, the additional VBM related to the Mn–Te bond reaches a maximum value, and the VBM related to the Pb–Te bond becomes very weak. Since substitutional adsorption is completed at a Mn thickness of about 0.45 ML, the whole 2nd layer is the $(\sqrt{3}\times\sqrt{3})R30^\circ$-$Pb_{0.67}Mn_{0.33}Te$ layer (see Fig. 2 and the above discussion), it can be deduced that the VBM related to the Pb–Te bond at an Mn thickness of 0.45 ML derives mainly from the outmost Pb–Te bilayer. For further deposition of Mn ($\Theta_{\mathrm{Mn}} > 0.45$ ML), the UPS spectra in Fig. 3 show clearly that a Fermi edge is detected, which results from the growth of metallic Mn islands, together with free Pb floating on top of the surface. With the Mn thickness increasing up to about 65 ML, the Fermi edge increases and becomes saturated due to the growth of metallic Mn islands.

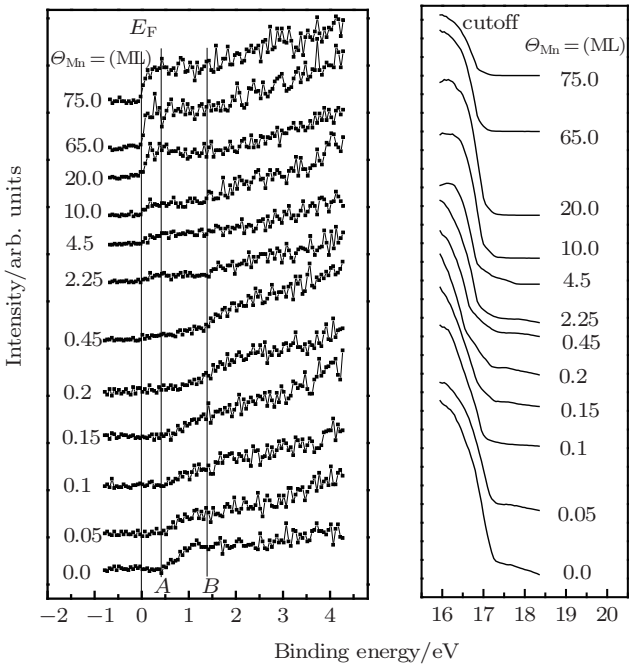


Fig. 3. Evolutions of UPS spectra with Mn thickness on PbTe (111), left panel: the valence-band structures; and right panel: the cutoff energies of the photoemissions. The VBM ascribed to pristine Pb–Te bond is marked by A, and the VBM ascribed to $(\sqrt{3}\times\sqrt{3})R30^\circ$-$Pb_{0.67}Mn_{0.33}Te$ is denoted by B.

According to the variation in the secondary cutoff energy with Mn thickness in Fig. 3, we can determine the change in work function. The change of work function with Mn thickness is shown in Fig. 4. With the Mn thickness increasing from 0.0 ML to 0.45 ML, the work function increases sharply from

3.95 eV to 4.35 eV (see the inset in Fig. 4).

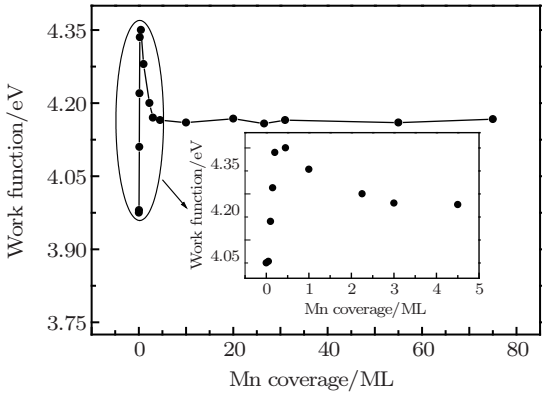


Fig. 4. Evolution of the work function with Mn thickness on PbTe (111). The inset shows the work function at low Mn thickness.

UPS and XPS measurements indicate that during the initial deposition of Mn ($\Theta_{\rm Mn} \leq 0.45$ ML), the Mn atoms are substituted for the 2nd layer Pb atoms by 'kicking them out' from the substrate, forming $(\sqrt{3}\times\sqrt{3})R30^\circ$-$Pb_{0.67}Mn_{0.33}Te$ at the 2nd layer, and the 'kicked out' Pb atoms are released to the top of the surface as free Pb atoms. The free Pb atoms floating on top of the surface will surely give rise to an increase in work function, however, its magnitude (4.25 eV for the metallic Pb[32]) does not increase enough to explain the increase in work function at the interface of Mn/PbTe (111). In general, at a semiconductor/metal interface, a downward band bending within the semiconductor layer will also lead to an increase in work function due to the space charge layer within the semiconductor.[33] However, the valence band spectra in Fig. 3 indicates that no band bending occurred at the Mn/PbTe (111) interface. Therefore, other mechanisms, i.e. the dipole layer due to surface polarization and charge transfer between Mn atom and the substrate, must be taken into consideration. For the clean Pb-terminated PbTe (111) substrate, Pb and Te layers are alternately arranged. As the electronegativity of Te is higher than that of Pb (2.1 for Te and 1.8 for Pb), the dipole layer at the outmost Pb–Te bilayer is formed by the surface polarization (see Fig. 2). For substitutional adsorption of Mn, our previous XPS measurements of the Te 3d core level (see Fig. 4(b) in Ref. [23]) show that the binding energy of the Te $3d_{5/2}$ core level shifts from 572.3 eV for the Pb–Te bond to 572.7 eV for the Mn–Te bond, which are drawn schematically in Fig. 5, suggesting that the outermost layer Te atoms at the substitutional atmosphere will lose more electrons than at the pristine Pb-terminated PbTe (111) atmosphere. This means that the surface depolarization will occur by substitutional adsorption of Mn. The surface depolarization, together with the free Pb floating on top of the surface, leads directly to the increase of the work function (from 3.95 eV to 4.35 eV). Further deposition of Mn with a thickness larger than 0.45 ML causes the work function to decrease sharply down to a saturated value of about 4.16 eV, which is comparable to the work functions of metallic Mn (4.1 eV) and Pb (4.25 eV).

Based on the XPS and UPS measurements, some Mn thickness values are of particular interest for determining the electronic structures at the Mn/PbTe (111) interface, and the energy level alignments at the interface are shown in Fig. 5. For an Mn thickness of 0 ML, the valence-band maximum is located at about 0.34 eV below the Fermi level ($E_{\rm F}$) (see Fig. 3). Considering a band gap of 0.32 eV at room temperature for PbTe, the Fermi level is almost pinned at the conduction band minimum (CBM), i.e. at 0.02 eV above the CBM. It suggests that the unsaturated electrons from the Pb atoms on the Pb-terminated surface directly result in a Fermi level shift into the conduction band.

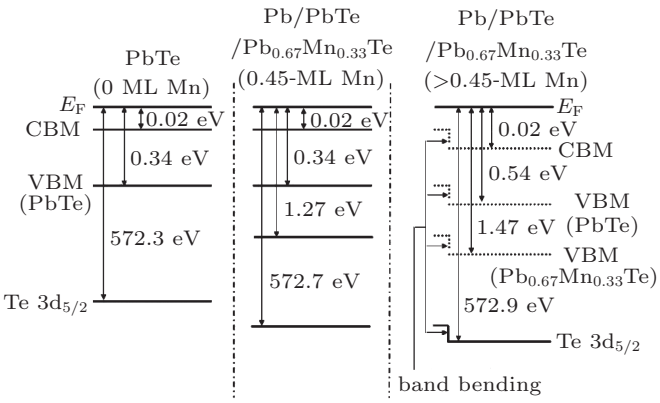


Fig. 5. Schematic energy level alignments for the Mn/PbTe (111) interface at different stages of pure PbTe (0.00 ML of Mn), the substituted $(\sqrt{3}\times\sqrt{3})R30^\circ$-$Pb_{0.67}Mn_{0.33}Te$ at the second layer (0.45-ML Mn), and the Pb/Mn covered substituted substrate (with a Mn thickness larger than 0.45 ML).

For an Mn thickness of 0.45 ML, a $(\sqrt{3}\times\sqrt{3})R30^\circ$-$Pb_{0.67}Mn_{0.33}Te$ layer at the 2nd layer is fully established, covered by a Pb–Te bilayer and free Pb at the outermost surface. Apparently, the formation of this surface structure leads to the appearance of a new VBM located at the 1.27 eV below the Fermi energy and a downward shift of the Te $3d_{5/2}$ core level by 0.4 eV (see Fig. 4(b) in Ref. [23]). This new VBM should be ascribed to the second $Pb_{0.67}Mn_{0.33}Te$ layer. For alloying of Mn with PbTe forming $Pb_{1-x}Mn_xTe$, the band gap $E_{\rm g}$ increases compared with the pure PbTe as a function of Mn concentration of x,[8] i.e., $E_{\rm g} = [(171.5+\sqrt{12.8^2+0.19(T+20)^2})+2500x]$ meV (where x is the Mn concentration and T is the temperature). For the $Pb_{0.67}Mn_{0.33}Te$ layer, the band gap is determined to be 1.14 eV at $T = 300$ K, which is roughly equal to the present experimental value of 1.25 eV, ($E_{\rm CBM} - E_{\rm VBM(Pb0.67Mn0.33Te)} = 1.25$ eV). First-principles calculations indicate that for this Mn substitutional $(\sqrt{3}\times\sqrt{3})R30^\circ$ superstructure, d-orbitals of Mn atoms are localized mainly at the valence band and are composed of p-orbitals of Te atoms without involvement with CBM composed of p-orbitals of Pb atoms at the Fermi level.[28] Therefore, no change of the CBM can be expected and the VBM of the top PbTe bilayer is also determined to be 0.02 eV below Fermi level (see the UPS measurements in Fig. 3).

For Mn deposition at a thickness beyond 0.45 ML, Mn nucleates on the substituted surface, forming metallic Mn islands, and those islands are covered with free Pb atoms on top of the surface. Of course, no changes in the band gap are expected once the substitutional adsorption has already been completed at an Mn thickness of 0.45 ML and the formation of a metallic Mn islands begins. However, our previous XPS measurements of the Te 3d core level (see Fig. 4(b) in Ref. [23]) show that in an intermediate Mn thickness of $0.45\ \text{ML} < \Theta_{\text{Mn}} < 7\ \text{ML}$, the Te $3d_{5/2}$ core level keeps shifting towards a high binding energy by about 0.2 eV (from 572.7 eV for 0.45-ML Mn to 572.9 eV for 7-ML Mn). As there is no evidence for the formation of a second, Te-containing species, it can be deduced that for an Mn thickness beyond 0.45 ML, the metallic Mn overlayer induces a downward band bending of about 0.2 eV within the underneath semiconducting substrate, and at a Mn thickness of 7 ML, the band bending is completely developed and remains constant for further Mn deposition. Considering this downward band bending of 0.2 eV in the intermediate Mn thickness, for the substituted substrate with the Pb-atoms-covered Mn islands, the positions of (virtual) CBM and VBM of the top PbTe bilayer are determined to be 0.22 eV and 0.54 eV below the Fermi level respectively, and the VBM of the $(\sqrt{3}\times\sqrt{3})R30^\circ$-$Pb_{0.67}Mn_{0.33}Te$ layer is located at 1.47 eV below the Fermi level. The whole process for Mn deposition on PbTe (111) shows an Ohmic contact forming at the Mn/PbTe (111) interface. An Ohmic contact at the Mn/CdTe (110) interface is also revealed by Dharmadasa *et al.*[32]

4. Conclusions

In this paper, we carry out the photoemission spectrum studies at the Mn/PbTe (111) interface. During the initial Mn deposition, subsurface substitutional adsorption of Mn occurs. With Mn thickness reaching up to about 0.45 ML, a $(\sqrt{3}\times\sqrt{3})R30^\circ$-$Pb_{0.67}Mn_{0.33}Te$ at the second layer, covered by free Pb atoms at the outmost surface, is formed. The work function of this substitutional interface is determined to be 4.35 eV, in comparison with the work function of 3.95 eV for the pristine PbTe (111) surface. The UPS measurements indicate that the valence band maximum associated with the $Pb_{0.67}Mn_{0.33}Te$ layer is located at 1.27 eV below the Fermi level. For further deposition of Mn, metallic Mn islands covered with free Pb atoms form at the top of the substitutional substrate, giving rise to 0.2 eV downward band bending: this band bending will result in the selective scattering of carriers with different energies, which is beneficial to the further improvement of the thermoelectric conversion efficiency for PbTe.[34] The results of the Mn/PbTe (111) interface behavior are of fundamental interest and also helpful to fabricate spintronics or spin-caloritronics based on PbTe, a well-known thermoelectric material with high tunneling magnetothermopower. We expect that the substitutional interface will yield interesting physics to be explored in comparison with the normal interface.

Acknowledgment

We thank Prof H. Z. Wu for the supply of the PbTe (111) substrate.

References

[1] Costi T A and Zlatic V 2012 *Phys. Rev. Lett.* **108** 036402
[2] Hochreiner A, Schwarzl T, Eibelhuber M, Heiss W, Springholz G, Kolkovsky V, Karczewski G and Wojtowicz T 2011 *Appl. Phys. Lett.* **98** 021106
[3] Si J X, Wu H Z, Xu T N, Cao C F and Huang Z C 2005 *Chin. Phys. Lett.* **22** 2353
[4] Xu T N, Wu H Z and Si J X 2008 *Acta Phys. Sin.* **57** 2574 (in Chinese)
[5] Galazka R R 1995 *J. Magn. Magn. Mater.* **140** 13
[6] Story T, Karczewski G, Swierkowski L and Galazkal R R 1990 *Phys. Rev. B* **42** 10477
[7] Dietl T and Spałek J 1983 *Phys. Rev. B* **28** 1548
[8] Osinniy V, Jedrzejczak A, Domuchowski W, Dybko K, Witkowska B and Story T 2005 *Acta Phys. Poloni. A* **108** 809
[9] Keiber T, Bridges F and Sales B C 2013 *Phys. Rev. Lett.* **111** 095504
[10] Zhang H, Luo J, Zhu H T, Liang J K, Ruan L M, Liu Q L, Li J B and Liu G Y 2012 *Acta Mater.* **60** 7241
[11] Hmooda A, Kadhim A and AbuHassan H 2013 *Mater. Sci. Semicond. Proc.* **16** 612
[12] Yang D J, Lu C G, Yin H M and Herman I P 2013 *Nanoscale* **5** 7290
[13] Rogacheva E I, Nashchekina O N, Grigorov S N, Us M A, Dresselhaus M S and Cronin S B 2003 *Nanotechnology* **14** 53
[14] Rogacheva E I, Nashchekina O N and Meriuts A V 2005 *Appl. Phys. Lett.* **86** 063103
[15] Lee P C, Chien C H, Dong G P, Huang W C, Chen C L, Tseng C M, Harutyunyan S R, Lee C H and Chen Y Y 2013 *Appl. Phys. Lett.* **103** 023115
[16] Heremans J P, Dresselhaus M S, Bell L E and Morelli D T 2013 *Nat. Nanotechnol.* **8** 471
[17] Buczko R and Cywinski Ł 2012 *Phys. Rev. B* **85** 205319
[18] Chen Y L, Chu J H, Analytis J G, Liu Z K, Igarashi K, Kuo H H, Qi X L, Moore S K, Lu D H, Hashimoto M, Sasagawa T, Zhang S C, Fisher I R, Hussain Z and Shen Z X 2010 *Science* **329** 659
[19] Wu H F, Zhang H J, Lu Y H, Si J X, Li H Y, Bao S N, Wu H Z and He P 2008 *Appl. Phys. Lett.* **92** 122112
[20] Hao S and Zhang Z 2007 *Phys. Rev. Lett.* **99** 166101
[21] Das R K, Tripathi G S and Misra P K 2005 *Phys. Rev. B* **72** 035216
[22] Łusakowski A and Dugaev V K 2005 *Phys. Rev. B* **71** 014422
[23] Wu H F, Zhang H J, Liao Q, Si J X, Li H Y, Bao S N, Wu H Z and He P 2010 *Surf. Sci.* **604** 882
[24] Wu H F, Zhang H J, Lu Y H, Xu T N, Si J X, Li H Y, Bao S N, Wu H Z and He P 2006 *J. Cryst. Growth* **294** 179
[25] Ueda S, Sekiyama A, Iwasaki T, Imada S, Suga S, Saitoh Y, Giriat W and Takeyama S 2008 *Phys. Rev. B* **78** 205206
[26] Bocquet A E, Mizokawa T, Saitoh T, Namatame H and Fujimori A 1992 *Phys. Rev. B* **46** 3771
[27] Sangaletti L, Verdini A, Pagliara S, Drera, G, Floreano L, Goldoni A and Morgante A 2010 *Phys. Rev. B* **81** 245320
[28] Wu H F, Wang Y, Lu Y H, Peng Y P and He P M 2013 *Appl. Surf. Sci.* **265** 120
[29] Headrick R L, Robinson I K, Vlieg E and Feldman L C 1989 *Phys. Rev. Lett.* **63** 1253
[30] Kitchen D, Richardella A, Tang J M, Flatté M E and Yazdani A 2006 *Nature* **442** 436
[31] Łusakowski A, Bogusławski P and Radzy'nski T 2011 *Phys. Rev. B* **83** 115206.
[32] Dharmadasa I M, Herrenden-Harker W G and Williams R H 1986 *Appl. Phys. Lett.* **48** 1802
[33] Horn K 2000 *Appl. Surf. Sci.* **166** 1
[34] Zhang Y C and Stucky G D 2014 *Chem. Mater.* **26** 837